Nanotechnology 35 (2024) 305201 (7pp) https://doi.org/10.1088/1361-6528/ad403f

Reduced interface effect of proton beam irradiation on the electrical properties of WSe_2/hBN field effect transistors

Seongmin Ko[1], Jiwon Shin[1], Juntae Jang[1], Jaeyong Woo[1], Jaeyoung Kim[1], Jaehyoung Park[1], Jongeun Yoo[1], Chongwu Zhou[2], Kyungjune Cho[3,*] and Takhee Lee[1,*]

[1] Department of Physics and Astronomy, and Institute of Applied Physics, Seoul National University, Seoul 08826, Republic of Korea
[2] Ming Hsieh Department of Electrical and Computer Engineering, University of Southern California, Los Angeles, CA 90089, United States of America
[3] Convergence Research Center for Solutions to Electromagnetic Interference in Future-mobility, Korea Institute of Science and Technology, Seoul 02792, Republic of Korea

E-mail: kcho@kist.re.kr and tlee@snu.ac.kr

Received 12 December 2023, revised 6 April 2024
Accepted for publication 18 April 2024
Published 7 May 2024

Abstract

Two-dimensional transition metal dichalcogenide (TMDC) semiconductors are emerging as strong contenders for electronic devices that can be used in highly radioactive environments such as outer space where conventional silicon-based devices exhibit nonideal characteristics for such applications. To address the radiation-induced interface effects of TMDC-based electronic devices, we studied high-energy proton beam irradiation effects on the electrical properties of field-effect transistors (FETs) made with tungsten diselenide (WSe_2) channels and hexagonal boron-nitride (hBN)/SiO_2 gate dielectrics. The electrical characteristics of WSe_2 FETs were measured before and after the irradiation at various proton beam doses of 10^{13}, 10^{14}, and 10^{15} cm^{-2}. In particular, we demonstrated the dependence of proton irradiation-induced effects on hBN layer thickness in WSe_2 FETs. We observed that the hBN layer reduces the WSe_2/dielectric interface effect which would shift the transfer curve of the FET toward the positive direction of the gate voltage. Also, this interface effect was significantly suppressed when a thicker hBN layer was used. This phenomenon can be explained by the fact that the physical separation of the WSe_2 channel and SiO_2 dielectric by the hBN interlayer prevents the interface effects originating from the irradiation-induced positive trapped charges in SiO_2 reaching the interface. This work will help improve our understanding of the interface effect of high-energy irradiation on TMDC-based nanoelectronic devices.

Supplementary material for this article is available online

Keywords: 2D devices, field effect transistor, proton beam irradiation, WSe_2, interface effect

1. Introduction

The space industry, fueled by human curiosity about outer space, has experienced notable growth over recent decades. Electrical engineering is integral to this progress, facing distinctive challenges due to the hostile space environment. Key issues include addressing the intense radiation in space and managing the substantial costs and weight limitations associated with launching spacecraft [1–3]. Conventional silicon-based transistors are increasingly unsuitable for space applications due to their vulnerability to radiation damage [4].

In response to these challenges, two-dimensional (2D) transition-metal dichalcogenides (TMDCs) have emerged as promising candidates as alternatives to silicon. Among those,

* Authors to whom any correspondence should be addressed.

tungsten diselenide (WSe_2) is widely studied as a TMDC semiconductor due to its ambipolar transporting characteristics having a layered structure, of which a single layer is approximately 0.7 nm thick [5, 6]. TMDC-based transistors are characterized by low power requirements and minimal thickness, offering potential weight reductions and enhanced radiation resistance [7–9]. Their inherent flexibility also paves the way for innovative design approaches, such as foldable kirigami or origami structures, which could further reduce overall costs [10–12].

For these reasons, there has been considerable research on the irradiation effects of TMDC transistors [8, 9, 13, 14]. Kim *et al* studied the changes in electrical characteristics of molybdenum disulfide field-effect transistors (FETs) irradiated with 10 MeV proton beams [8]. Similarly, Shin *et al* reported on the irradiation effects of WSe_2 FETs exposed to 10 MeV proton beams [14]. Table S1 in the supplementary material summarizes the studies regarding the irradiation effects on TMDC-based devices. These studies, among others, have shown that the electrical characteristics of TMDC-based FETs change upon proton irradiation, but the changes are attributed to effects on parts such as SiO_2 dielectric other than the TMDC channel, indicating that the TMDC itself is more resistant to radiation compared to silicon [8, 14, 15]. However, to our knowledge, none of these studies have specifically isolated the effects from the interface that the TMDC channel forms with other parts. Given that 2D materials have a larger surface-to-volume ratio compared to conventional three-dimensional materials, they are significantly influenced by interface effects. Therefore, it is essential to separate effects originating from the interface to properly investigate TMDC irradiation effects.

In this work, we examined the effects of high-energy proton beam irradiation of WSe_2 FETs, incorporating a hexagonal boron nitride (hBN) interlayer between the SiO_2 dielectric and the WSe_2 channel to suppress such interface effects [16]. By varying the thickness of the hBN interlayer, we also investigated whether the separation distance between SiO_2 and WSe_2 affects the irradiation effect on the FETs. We found out that the hBN interlayer effectively suppressed the interface effect of the proton beam irradiation when the hBN layer was sufficiently thick to separate the SiO_2 dielectric far enough from the WSe_2 channel. Our results provide a deeper understanding of the interface effects of 2D semiconductors under harsh conditions like radiation and pave the way for the application of 2D materials in future space electronics.

2. Experiment

To investigate the influence of hBN thickness on the effect of proton irradiation and their interface effects, we fabricated two types of FETs with different hBN interlayer thicknesses: one ranging between 20 and 30 nm (denoted as thin hBN) and another between 90 and 110 nm (denoted as thick hBN). The schematic image in figure 1(a) shows a WSe_2/hBN heterostructure back-gated FET fabricated on a p++ Si (highly boron-doped silicon) substrate with a 270 nm SiO_2 layer. We transferred mechanically exfoliated WSe_2 flakes onto desired hBN flakes by using the dry transfer technique. We used WSe_2 flakes with a thickness of 2–10 nm in this study, which are 3–14 layers thick. Source and drain contact electrodes were patterned by e-beam lithography, followed by depositing Ti (5 nm thick)/Au (50 nm thick) using electron beam evaporation. Lastly, to avoid unwanted effects from environments during electrical characterizations and proton beam irradiation, we encapsulated the FETs with an additional hBN layer (~15 nm thick). Figure 1(b) shows an optical image of a hBN/WSe_2/hBN heterostructure FET. The encapsulation was particularly necessary since the electrical properties could be inevitably altered by the ambient environment. The thicknesses of the hBN and WSe_2 flakes were confirmed using atomic force microscopy (NX 10 AFM, Park Systems), as shown in figure 1(c) and figure S1 in the supplementary material.

We then annealed the fabricated devices at 200 °C for an hour in a vacuum (~10^{-2} Torr) and consecutively characterized their electrical properties, such as the transfer characteristic curves (drain-source current versus gate voltage; $I_{DS}-V_{GS}$) of the FETs, using a semiconductor parameter analyzer (Keithley 4200 SCS) in a vacuum probe station (MS Tech M6VC). Then, each FET was irradiated with a proton beam with an energy of 10 MeV using the MC-50 cyclotron at the Korea Institute of Radiological and Medical Sciences, as shown in figures 1(d) and (e). Three different doses of proton beam were irradiated to devices: 10^{13}, 10^{14}, and 10^{15} cm^{-2}, with each dose applied to both types of devices with thin and thick hBN layers. The irradiation area was as large as a few square centimeters so that it could cover the entire devices and substrates. After the proton irradiation, we annealed FETs again and measured the electrical characteristics of the proton-irradiated devices under the same measurement conditions.

3. Results and discussion

Figure 2 shows the changes in the transfer characteristics of FETs with thin and thick hBN interlayers before and after the proton beam irradiations under different dose conditions. The representative thin and thick hBN devices are presented in figures 2(a) and (e), respectively, showing ambipolar transistor behaviors. For all proton doses, we could observe a threshold voltage shift in the transfer curve to a certain direction before and after proton beam exposure. According to a previously reported study, when a proton beam was irradiated to WSe_2 FETs without hBN interlayers, doses of 10^{14} cm^{-2} or below induced a negative threshold voltage shift, but at a higher dose, a positive threshold voltage shift occurred. These phenomena were explained by the irradiation-induced positive oxide traps in the gate dielectric that can generate additional electric field to the devices at low proton dose conditions. On the other hand, under a high irradiation dose condition, electron trapping at the interface between SiO_2 and WSe_2 could be promoted, resulting in the threshold voltage shift to the positive direction [14].

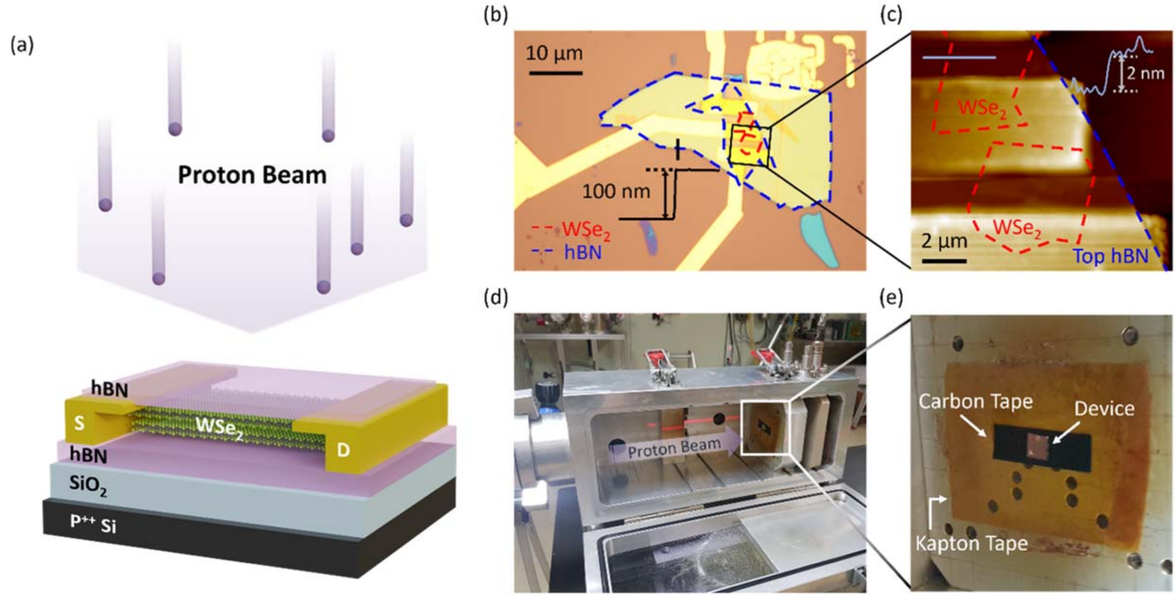

Figure 1. (a) A schematic of a fabricated device irradiated with a proton beam. S and D mean source and drain electrodes made with Ti/Au, respectively. (b) An optical image of a WSe_2/hBN FET with WSe_2 channels (red dotted lines) on a 100 nm-thick bottom hBN layer (outer blue dotted line). The device is encapsulated with a top hBN layer (inner blue dotted line). The inset shows the thickness of the bottom hBN layer, measured with AFM. (c) AFM image of the zoomed-in area in (b) with a cross-sectional height profile of a WSe_2 flake. (d) An image of the chamber where protons are irradiated to the devices, with (e) a zoomed-in image of the mounted device.

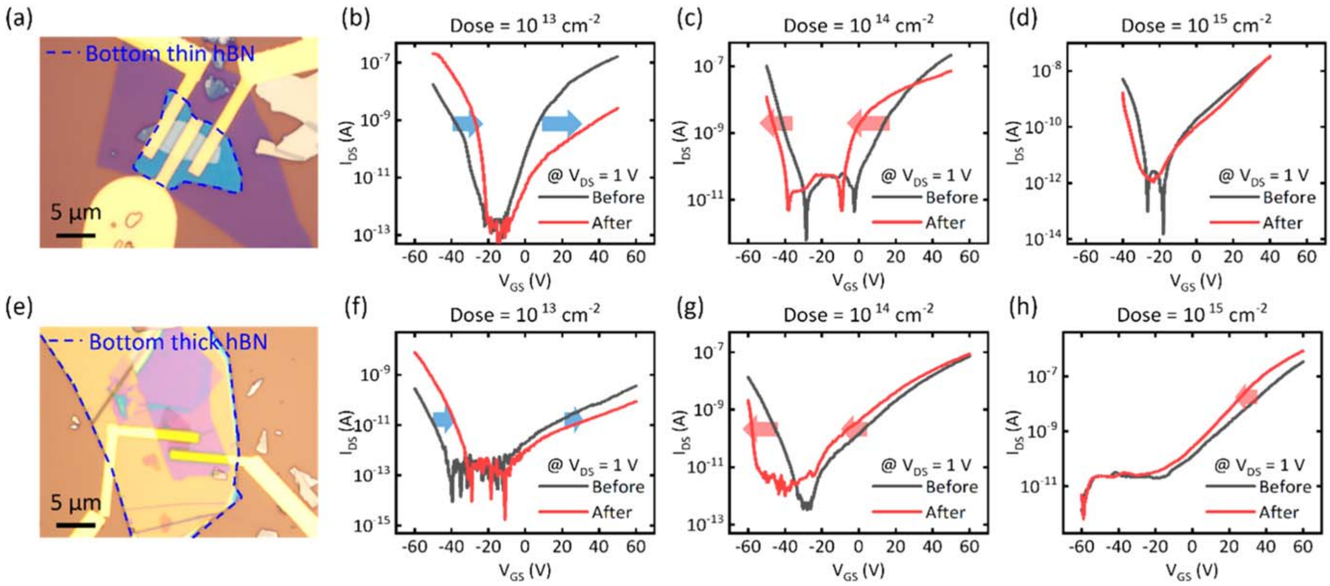

Figure 2. Optical images of WSe_2/hBN FETs and their transfer curves before and after proton beam irradiation. (a) An optical image of a device with a thin hBN layer (typical thickness of 20–30 nm) and the transfer curves of WSe_2 FETs with thin hBN layers before and after the irradiation with a proton beam dose of (b) $10^{13}\ cm^{-2}$, (c) $10^{14}\ cm^{-2}$, and (d) $10^{15}\ cm^{-2}$. (e) An optical image of a device with a thick hBN layer (typical thickness of 90–110 nm) and the transfer curves of WSe_2 FETs with thick hBN layers before and after the irradiation with a proton beam dose of (f) $10^{13}\ cm^{-2}$, (g) $10^{14}\ cm^{-2}$, and (h) $10^{15}\ cm^{-2}$. All measurements for (b–d) and (f–h) are done under the voltage drop between the source and drain electrodes of 1 V.

Likewise, for WSe_2/hBN heterostructure FETs, as shown in figures 2(c) and (g), a dose of $10^{14}\ cm^{-2}$ resulted in a negative shift of the threshold voltage, irrespective of hBN layer thickness, which is a similar result to the case of low-dose proton irradiated WSe_2 FETs without hBN layers since this is due to the additional electric field by irradiation-induced positive oxide-trapped charges in the SiO_2 layer. However, under a high dose of $10^{15}\ cm^{-2}$, the FETs with a thin hBN layer showed a negligible threshold voltage shift (figure 2(d)), while the ones with a thick hBN layer kept exhibiting a noticeable negative threshold voltage shift (figure 2(h)). It should be noted that WSe_2 FETs without hBN interlayers showed a positive threshold voltage shift after a high dose of $10^{15}\ cm^{-2}$ irradiation [14]. This can be inferred that the addition of a sufficiently thick hBN layer could prevent the electron trapping effect at the interface with SiO_2

at high proton irradiation doses. The output curves for the cases of $10^{15}\,cm^{-2}$ dose are shown in figure S2 in the supplementary material, which further supports the suppressing effect of hBN. More details will be discussed later. Meanwhile, we could observe increased drain current at positive V_{GS} and decreased current at negative V_{GS} in both thin and thick hBN interlayer devices when the dose was $10^{13}\,cm^{-2}$ (figures 2(b) and (f)), which may be attributed to the oxidation of the channel. It has been known that WSe_2 FETs are prone to oxidation under ambient conditions at moderate temperatures, resulting in similar transfer characteristic changes [17, 18], and the encapsulation may not be perfect because we transferred the top hBN layer after the deposition of metal electrodes. We also confirmed that separate measurements on a control device with a thick hBN layer, which was fabricated and treated identically but without proton irradiation, showed a similar drain current change (figure S3 in the supplementary material). Given this, it is inferred that the current changes in WSe_2 FETs irradiated with a proton beam with a dose of $10^{13}\,cm^{-2}$, irrespective of hBN thickness, arose because the effect of the irradiation-induced negative threshold voltage shift was overshadowed by the oxidation effect.

To quantitatively analyze the effect of proton irradiation on WSe_2/hBN FETs, we evaluated the change in threshold voltage after irradiation (ΔV_{TH}) and the drain-source current ratio between before and after irradiation (I_{after}/I_{before}) in the electron accumulation region for different proton doses and hBN thicknesses. Particularly, when calculating the current ratio, the values of V_{GS} were chosen accordingly for different hBN thicknesses to ensure an equal gate electric field across the WSe_2 channels. The V_{TH} value was determined by the *x*-intercept of the tangent line at the point with maximum transconductance. Error bars are presented in figure 3 only when multiple devices (typically, 2–3 devices) were measured at each condition of dose or hBN layer thickness. Note that we were not able to conduct many experiments due to various limitations such as device fabrication and the proton-irradiation facility access.

For WSe_2 FETs with thin hBN interlayers, as shown in figure 3(a), V_{TH} further shifted to a negative gate voltage direction as the proton dose increased from 10^{13} to $10^{14}\,cm^{-2}$. However, at a proton dose of $10^{15}\,cm^{-2}$, V_{TH} shifted positively and ΔV_{TH} increased to a value similar to that for the $10^{13}\,cm^{-2}$ dose case. These are similar results reported for WSe_2 FETs without hBN layers [14], but the positive shift of V_{TH} at the $10^{15}\,cm^{-2}$ proton dose for WSe_2 FETs with thin hBN layers is less drastic. Regarding the current ratio shown in figure 3(b), the current ratio at the $10^{15}\,cm^{-2}$ proton dose case was similar to that of the $10^{14}\,cm^{-2}$ dose case, which is different from the trend from low doses where the current ratio increased as the dose increased from 10^{13} to $10^{14}\,cm^{-2}$. In short, there is a trend change in both ΔV_{TH} and I_{after}/I_{before} values between low and high doses of proton irradiation, but the change was smaller compared to that of one without hBN.

However, for WSe_2 FETs with thick hBN layers, as shown in figure 3(c), the trend that V_{TH} shifts even further to a negative direction as the dose increases remained unchanged even at a high dose of $10^{15}\,cm^{-2}$, indicating that the factor which made V_{TH} shift positively for the case of WSe_2 FETs without hBN layers at the high dose of $10^{15}\,cm^{-2}$ could be prevented by the introduction of a thick hBN layer. Also, this contrasts with the behavior observed in WSe_2 FETs with thin hBN layers (figure 3(a)), which suggests that the hBN layer should be thick enough to properly prevent the positive V_{TH} shift due to the charge trapping at the interface. This pattern was also evident in the current ratios, as shown in figure 3(d), i.e. the current ratio consistently increased as the dose increased up to $10^{15}\,cm^{-2}$.

In particular, to understand how the hBN layer and its thickness influence the trend of ΔV_{TH} at the high dose of $10^{15}\,cm^{-2}$, it is essential to understand the behavior of irradiated protons as they pass through the device. When the devices are exposed to a proton beam, the protons lose energy as they penetrate through the device and eventually stop at a certain point called the 'stopping position', where they release most of their energy [1, 19]. Using the stopping and range of ions in matter (SRIM) simulation, we could approximately determine this stopping position [20]. As figure S7 in the supplementary material shows, the stopping position for protons in the WSe_2/hBN heterostructure FETs used in this study was estimated to be $\sim$700 μm, while the device itself is approximately 500 μm thick. This indicates that nearly all the protons can pass through the FETs without dissipating much energy to the WSe_2 and hBN layers. Thus, in these FETs, the SiO_2 layer is most affected by the proton beam and the electrical properties of the WSe_2 channel itself possibly remain unchanged by proton irradiation of 10 MeV [14]. According to previous studies, it has been known that irradiated protons generate electron–hole pairs as they penetrate through the SiO_2 layer. The electrons, which have higher mobility than the holes, are quickly swept away within a picosecond or less [21]. On the other hand, while some holes recombine with electrons, other holes stay nearby where they were created and are trapped in the SiO_2 layer [22, 23]. These irradiation-induced positively charged oxide-trapped holes (denoted as positive oxide-trapped charges) apply a positive gate bias to the WSe_2 channel, resulting in a negative threshold voltage shift. For WSe_2 FETs without hBN layers irradiated with a moderate dose (i.e. $10^{14}\,cm^{-2}$) of the proton beam, the effect from irradiation-induced positive oxide-trapped charges in the SiO_2 layer is dominant, leading to a negative threshold voltage shift. Meanwhile, a partial number of irradiation-induced positive oxide-trapped charges can move to the interface of the SiO_2 layer via hopping transport through localized states in SiO_2, and be trapped at the interface between the channel and dielectric. In bare WSe_2 FETs without an hBN layer where the SiO_2 layer and WSe_2 channel are directly in contact, the irradiation-induced positive trapped charges at the SiO_2 interface can cause the formation of a layer of electron trapping sites in the channel near the interface, causing a positive threshold voltage shift. At a higher proton dose, this effect was found to be dominant over the gate modulation effect from the irradiation-induced positive oxide-trapped charges in the SiO_2 layer [14].

In WSe_2/hBN FETs with thin hBN layers, the threshold voltage shifts depending on irradiation doses behave similarly to the case for bare WSe_2 FETs (figures 3(a) and (b)).

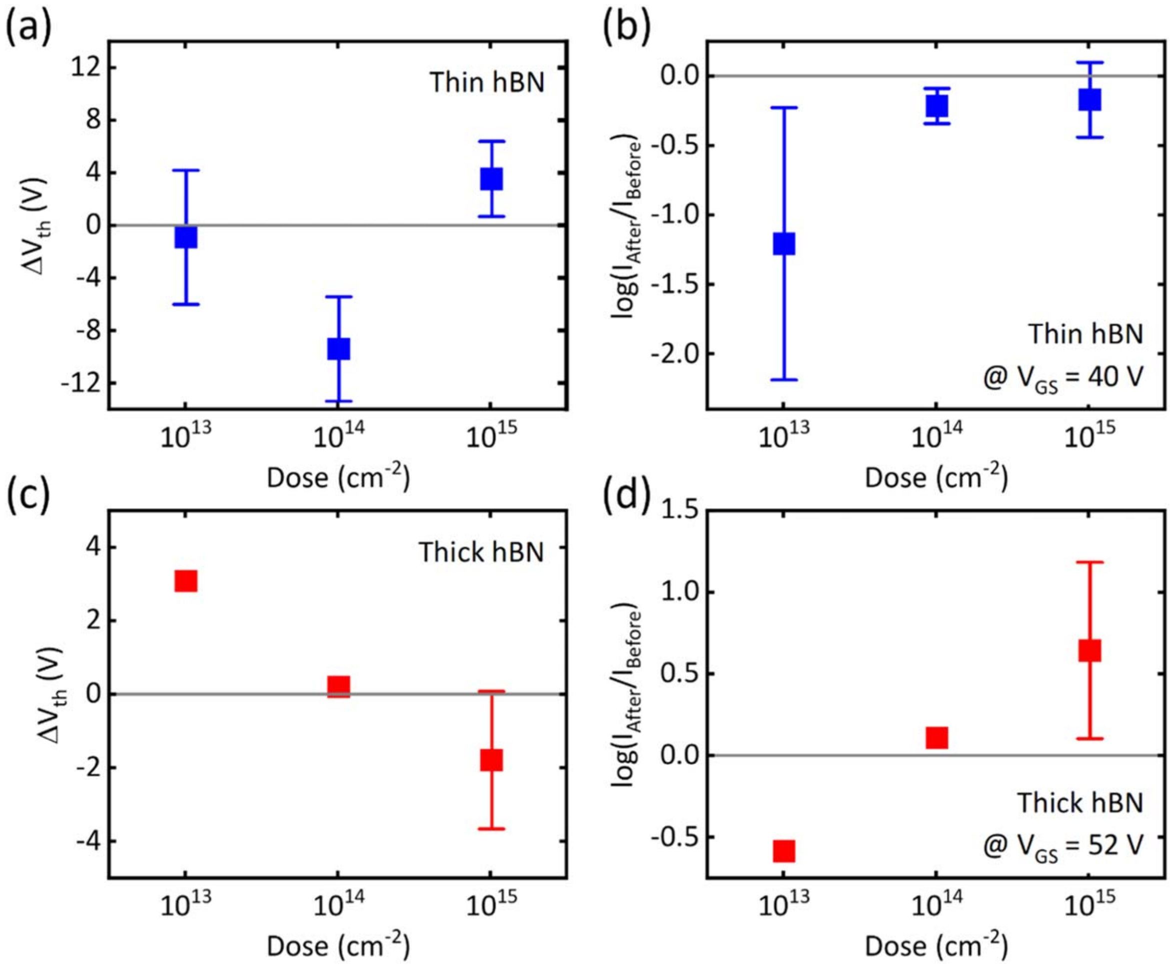

Figure 3. (a) Threshold voltage changes (ΔV_{th}) and (b) current ratio ($\log(I_{After}/I_{Before})$) at $V_{GS} = 40$ V of WSe_2 FETs with thin hBN layers. (c) ΔV_{th} values and (d) $\log(I_{After}/I_{Before})$) values at $V_{GS} = 52$ V of WSe_2 FETs with thick hBN layers.

However, in WSe_2/hBN FETs with thick hBN layers, the positive threshold voltage shift caused by the interface-trap sites was not apparent and only the negative shift caused by the positive oxide-trapped charges in the SiO_2 bulk layer was evident even at the high dose condition (figures 3(c) and (d)). This result can be explained by the effect of a thick hBN layer preventing positive oxide-trapped charges from reaching the WSe_2/hBN interface by physically separating SiO_2 and WSe_2. Figures 4(a)–(c) show the schematics of proton-irradiated WSe_2 FETs with thin hBN. For the irradiation-induced positive oxide-trapped charges to cause a positive shift in threshold voltage, they should reach the WSe_2/hBN interface past the hBN layer and form electron trap sites in the channel at the interface. It is possible that some of the irradiation-induced oxide-trapped charges generated in SiO_2 migrate into hBN via hopping transport through defects in the hBN [24, 25], reaching the WSe_2/hBN interface. For FETs with thin hBN, at the low proton dose conditions (figure 4(b)), the effect of the positive oxide-trapped charges in the SiO_2 bulk is dominant, whereas, at the high proton dose condition, some positive oxide-trapped charges in the SiO_2 bulk can reach the WSe_2/hBN interface, causing the positive shift in threshold voltage (figure 4(c)). Meanwhile, for FETs with thick hBN, the phenomenon is similar at the low proton dose conditions (figure 4(e)), but even the high dose condition of 10^{15} cm^{-2} is insufficient for a part of positive oxide-trapped charges to reach the WSe_2/hBN interface, thus the effect of gate modulation from the positive oxide-trapped charges in the SiO_2 bulk can be dominant (figure 4(f)). Thus, the interface effect weakens when the distance between the WSe_2 channel and the SiO_2 layer is larger, which is when the hBN layer is thicker. In summary, more electron trap states could be formed in the WSe_2/hBN interface of thin hBN FETs than in thick hBN FETs as shown in figures 4(c) and (f). Note that the idea that irradiation-induced positive oxide-trapped charges can transport into the hBN layer also explains the abnormal current lowering of proton-irradiated FETs with thin hBN shown at high positive V_{GS} (figure 2(c)). Irradiation-induced oxide-trapped charges can migrate following the applied gate voltage [22, 23, 26]. Thus, when a strong positive gate voltage is applied to the FETs, more holes may migrate to the WSe_2/hBN interface, forming electron trap sites in the channel interface, thereby hindering electron transportation in the channel. This effect was much less apparent for FETs with thick hBN (figures 2(g) and (h)), because the hBN was too thick for holes to migrate to the interface, thereby enhancing the resilience of 2D van der Waals material-based electronic devices against high-energy beam irradiation.

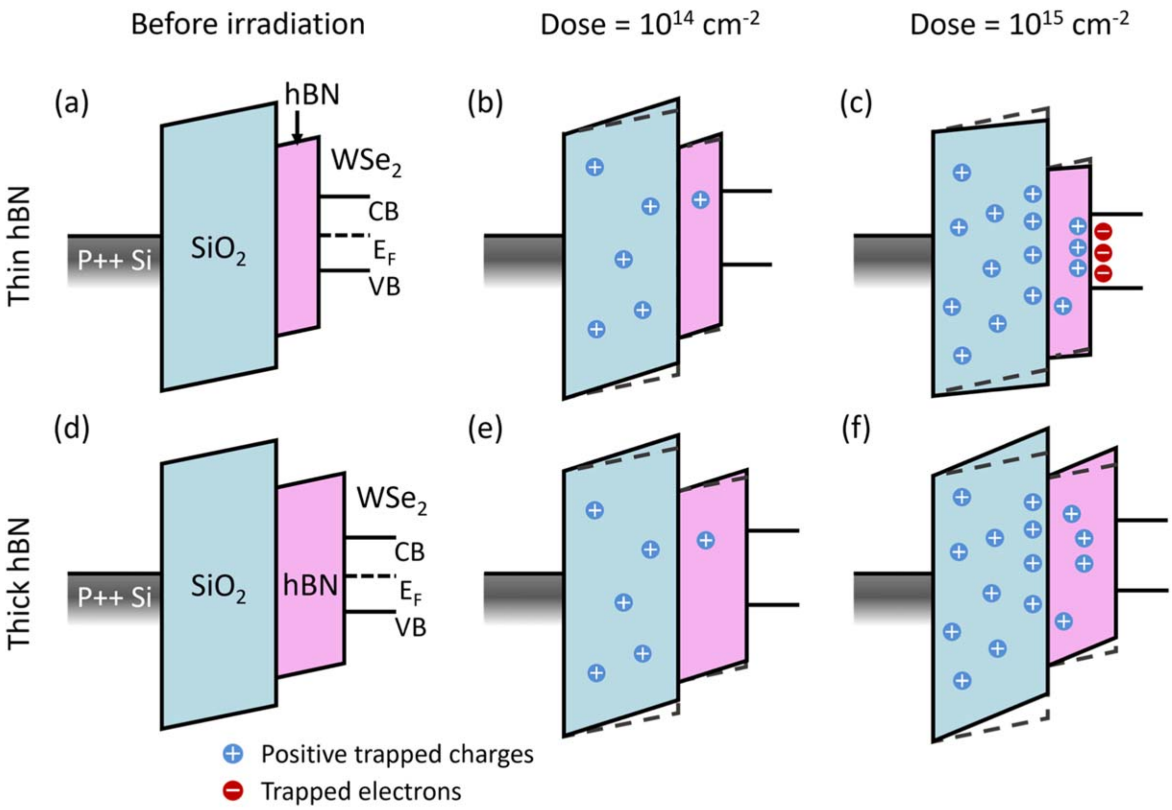

Figure 4. Band diagrams of the devices irradiated with proton beams. Cases before irradiation are shown for devices with (a) thin hBN and (b) thick hBN layers. Cases after proton irradiation with 10^{14} cm^{-2} proton dose for devices with (c) thin hBN and (d) thick hBN layers. Cases after proton irradiation with 10^{15} cm^{-2} proton dose for devices with (c) thin hBN and (d) thick hBN layers.

4. Conclusion

We examined the effect of high-energy proton beam irradiation on WSe_2/hBN heterostructure FETs. For FETs with thick hBN layers, the transfer curve consistently shifted in the negative direction across all irradiation doses, while the threshold voltage shifted positively under a high dose of proton irradiation (10^{15} cm^{-2}) for FETs with thin hBN layers. This is because hBN separates the WSe_2 channel and the SiO_2 dielectric so that fewer irradiation-induced positive oxide-trapped charges can transport to the WSe_2/hBN interface and form electron trap sites. The sufficiently thick hBN layer can prevent the positive threshold voltage shift arising from the interface effect. Our study advances the understanding of the impact of proton beam irradiation on 2D TMDC-based devices. It highlights the potential of hBN as an interlayer for mitigating irradiation-induced effects. This finding is pivotal in realizing reliable, 2D-based electronic applications capable of withstanding harsh environments.

Acknowledgments

The authors appreciate the financial support of the National Research Foundation of Korea (NRF) Grants (No. 2021R1A2C3004783 and No. RS-2023-00220471) funded by the Ministry of Science and ICT (MSIT) of Korea. KC appreciates the support of the NRF grant funded by MSIT (No. 2021R1C1C2091728) and the National Research Council of Science & Technology (NST) Grant (CRC22031-000). We are thankful for the beam time grants from the proton beam facilities of the Korea Institute of Radiological and Medical Sciences.

Data availability statement

All data that support the findings of this study are included within the article (and any supplementary files).

ORCID iDs

Takhee Lee https://orcid.org/0000-0001-5988-5219

References

[1] Claeys C 2002 *Radiation Effects in Advanced Semiconductor Materials and Devices* (Springer) (https://doi.org/10.1007/978-3-662-04974-7)

[2] Peck D S and Schmid E R 1963 Effects of radiation on transistors in the first telstar satellite *Nature* **199** 741–4

[3] Williams I and Dahlgren M 2022 *Boost-Phase Missile Defense: Interrogating the Assumptions* (Center for Strategic and International Studies) (https://scholar.google.com/scholar_lookup?title=Boost-Phase+Missile+Defense:

+Interrogating+the+Assumptions&author=Williams,+I.&author=Dahlgren,+M.&publication_year=2022)
[4] Secretariat E 2008 Methods for the calculation of radiation received and its effects, and a policy for design margins *European Cooperation for Space Standardization, Noordwijk* (https://radconsult.eu/pages/radlinks/radlinks.html)
[5] Das S and Appenzeller J 2013 WSe_2 field effect transistors with enhanced ambipolar characteristics *Appl. Phys. Lett.* **103** 103501
[6] Kalikhman V L and Ya S U 1973 Transition-metal chalcogenides with layer structures and features *Sov. Phys. Usp.* **15** 728
[7] Radisavljevic B, Radenovic A, Brivio J, Giacometti V and Kis A 2011 Single-layer MoS_2 transistors *Nat. Nanotechnol.* **6** 147–50
[8] Kim T-Y, Cho K, Park W, Park J, Song Y, Hong S, Hong W-K and Lee T 2014 Irradiation effects of high-energy proton beams on MoS_2 field effect transistors *ACS Nano* **8** 2774–81
[9] Schranghamer T F, Pannone A, Ravichandran H, Stepanoff S P, Trainor N, Redwing J M, Wolfe D E and Das S 2023 Radiation resilient two-dimensional electronics *ACS Appl. Mater. Interfaces* **15** 26946–59
[10] Zhang Z, Tian Z, Mei Y and Di Z 2021 Shaping and structuring 2D materials via kirigami and origami *Mater. Sci. Eng.: R: Rep.* **145** 100621
[11] Blees M K *et al* 2015 Graphene kirigami *Nature* **524** 204–7
[12] Chen H *et al* 2019 Atomically precise, custom-design origami graphene nanostructures *Science* **365** 1036–40
[13] Arnold A J, Shi T, Jovanovic I and Das S 2019 Extraordinary radiation hardness of atomically thin MoS_2 *ACS Appl. Mater. Interfaces* **11** 8391–9
[14] Shin J, Cho K, Kim T-Y, Pak J, Kim J-K, Lee W, Kim J, Chung S, Hong W-K and Lee T 2019 Dose-dependent effect of proton irradiation on electrical properties of WSe_2 ambipolar field effect transistors *Nanoscale* **11** 13961–7
[15] Huang X-N, Shi J-Y, Yao Y, Peng S-A, Zhang D-Y and Jin Z 2021 Layer thickness influenced irradiation effects of proton beam on MoS_2 field effect transistors *Nanotechnology* **32** 135204
[16] Lee C, Rathi S, Khan M A, Lim D, Kim Y, Yun S J, Youn D-H, Watanabe K, Taniguchi T and Kim G-H 2018 Comparison of trapped charges and hysteresis behavior in hBN encapsulated single MoS_2 flake based field effect transistors on SiO_2 and hBN substrates *Nanotechnology* **29** 335202
[17] Liu B, Ma Y, Zhang A, Chen L, Abbas A N, Liu Y, Shen C, Wan H and Zhou C 2016 High-performance WSe_2 field-effect transistors via controlled formation of in-plane heterojunctions *ACS Nano* **10** 5153–60
[18] Yamamoto M, Dutta S, Aikawa S, Nakaharai S, Wakabayashi K, Fuhrer M S, Ueno K and Tsukagoshi K 2015 Self-limiting layer-by-layer oxidation of atomically thin WSe_2 *Nano Lett.* **15** 2067–73
[19] Messenger S R, Burke E A, Summers G P, Xapsos M A, Walters R J, Jackson E M and Weaver B D 1999 Nonionizing energy loss (NIEL) for heavy ions *IEEE Trans. Nucl. Sci.* **46** 1595–602
[20] Ziegler J F and Biersack J P 1985 *Treatise on Heavy-Ion Science: Volume 6: Astrophysics, Chemistry, and Condensed Matter* ed D A Bromley (Springer) 93–129
[21] Hughes R C 1973 Charge-carrier transport phenomena in amorphous SiO_2: direct measurement of the drift mobility and lifetime *Phys. Rev. Lett.* **30** 1333–6
[22] Oldham T R and McLean F B 2003 Total ionizing dose effects in MOS oxides and devices *IEEE Trans. Nucl. Sci.* **50** 483–99
[23] Oldham T R 1999 *Ionizing Radiation Effects in MOS Oxides* (World Scientific) (https://doi.org/10.1142/3655)
[24] Wu X, Ge R, Chen P-A, Chou H, Zhang Z, Zhang Y, Banerjee S, Chiang M-H, Lee J C and Akinwande D 2019 Thinnest nonvolatile memory based on monolayer h-BN *Adv. Mater.* **31** 1806790
[25] Jeong H, Kim J, Kim D Y, Kim J, Moon S, Ngome Okello O F, Lee S, Hwang H, Choi S-Y and Kim J K 2020 Resistive switching in few-layer hexagonal boron nitride mediated by defects and interfacial charge transfer *ACS Appl. Mater. Interfaces* **12** 46288–95
[26] Schwank J, Winokur P, McWhorter P, Sexton F, Dressendorfer P and Turpin D 1984 Physical mechanisms contributing to device 'rebound' *IEEE Trans. Nucl. Sci.* **31** 1434–8